

Fabrication of nanochannels on polystyrene surface

Ran Peng and Dongqing Li

Citation: *Biomicrofluidics* **9**, 024117 (2015); doi: 10.1063/1.4918643

View online: <http://dx.doi.org/10.1063/1.4918643>

View Table of Contents: <http://scitation.aip.org/content/aip/journal/bmf/9/2?ver=pdfcov>

Published by the [AIP Publishing](#)

Articles you may be interested in

[Effects of surface oxide layer on nanocavity formation and silver gettering in hydrogen ion implanted silicon](#)

J. Appl. Phys. **114**, 023502 (2013); 10.1063/1.4812736

[Surface modification by subsurface pressure induced diffusion](#)

Appl. Phys. Lett. **100**, 041908 (2012); 10.1063/1.3679616

[Nanopatterning of Si surfaces by normal incident ion erosion: Influence of iron incorporation on surface morphology evolution](#)

J. Appl. Phys. **109**, 104315 (2011); 10.1063/1.3585796


[A surface diffusion model for Dip Pen Nanolithography line writing](#)

Appl. Phys. Lett. **96**, 243105 (2010); 10.1063/1.3454777

[Three-dimensional micronanofabrication via two-photon-excited photoisomerization](#)

Appl. Phys. Lett. **95**, 083118 (2009); 10.1063/1.3213351

How to Simulate & Design Microfluidics Devices



Fabrication of nanochannels on polystyrene surface

Ran Peng and Dongqing Li^{a)}

*Department of Mechanical and Mechatronics Engineering, University of Waterloo,
Waterloo, Ontario N2L 3G1, Canada*

(Received 2 February 2015; accepted 8 April 2015; published online 17 April 2015)

Solvent-induced nanocrack formation on polystyrene surface is investigated experimentally. Solubility parameter and diffusion coefficient of alcohols are employed to elucidate the swelling and cracking processes as well as the crack size. Experimental results show that the crack size increases with the heating temperature, heating time, and the concentration and volume of the alcohols. A guideline on fabricating single smaller nanocracks on polymers by solvent-induced method is provided. Nanocracks of approximately 64 nm in width and 17.4 nm in depth were created and replicated onto PDMS (polydimethylsiloxane) slabs to form nanochannels. © 2015 AIP Publishing LLC. [<http://dx.doi.org/10.1063/1.4918643>]

I. INTRODUCTION

Fabrication of nanochannels with at least one dimension smaller than 200 nm is a key to the studies of nanofluidics. Various nanofluidic systems have been developed in recent years to investigate transport phenomena unique in nanoscale, such as surface charge governed ion enrichment;^{1–3} and biological applications including DNA stretching, detecting and separation;^{4–6} as well as water purification and energy conversion.^{7,8} However, the factors limiting the development of nanofluidics include the sophisticated equipment, complicated procedure, and high cost of the nanofabrication techniques.

To date, various methods have been developed for fabricating nanochannels. Electron beam lithography (EBL)^{9,10} and focused ion beam lithography (FIB)^{11,12} have a resolution as high as few nanometers; however, they are time-consuming and expensive. Deep-UV or X-ray lithography,^{13,14} interferometric lithography (IL),¹⁵ and nanoimprint lithography (NIL)¹⁶ are cost less and are more productive than EBL and FIB; however, these methods highly depend on the expensive masks. Combining with the lithography methods mentioned above, etching and deposition techniques are applied to do the post processes to transfer the nano-patterns to silicon wafers or glass surfaces.^{17,18} The etching and deposition systems are complicated and it is hard to control the etching and deposition speed and direction precisely. Nanomaterials such as nanowires, nanotubes, nano-membranes, and nanofibers, with a feature size down to few nanometers, have been widely leveraged to make nanofluidic systems.^{19–21} These nanomaterial-assisted methods are cost-effective and simple; however, the alignment is the biggest challenge during the fabrication process, because the size of the nanowires is too small to be manipulated by mechanical tools.

Collapsing of elastomeric material has been applied to create nanochannels. Park and Huh²² fabricated nanochannels with a feature size as small as 60 nm by utilizing the collapse of PDMS (polydimethylsiloxane) roof of a microchannel. Nanochannel mask fabrication by combining the roof collapse with the standard photolithography has also been reported.²³ A tunable elastomeric nanochannel fabrication method was presented by Huh *et al.*²⁴ Kim *et al.*²⁵ reported a simple triangular nanochannel fabrication method by incomplete bonding a PDMS slab to a glass slide. Sivanesan *et al.*²⁶ created nanochannels with 100 nm in diameter based on thermal deformation of rigid polycarbonate (PC) substrates. Another simple method called

^{a)} Author to whom correspondence should be addressed. Electronic mail: dongqing@uwaterloo.ca.

Microchannel refilling (MR) was developed by Li *et al.*²⁷ Grimes *et al.*²⁸ reported a new method to fabricate nanochannels by leveraging shrinkage property of thermoplastics. These methods are easy to perform; however, the biggest problems are the reproducibility and the difficulty to control the fabrication process.

To overcome these problems, it is desirable to develop methods that are simple, cost-effective, controllable, reproducible, and allowing easy integration of nanochannels with microchannels. Creation of cracks or wrinkles on PDMS surfaces by treating PDMS with oxygen plasma^{29,30} has potential to generate nanopatterns. However, the crack size is too large to form a nanochannel and is too sensitive to the externally applied force, which results in a poor reproducibility. Xu *et al.*³¹ improved the crack method by utilizing solvent-induced cracking. In his work, a certain volume of pure ethanol was placed in a polystyrene petri-dish and covered with a petri-dish lid. During the heating process, the ethanol was vaporized and condensed into liquid form on the petri dish lid inner surface. As a result, the ethanol will swell the lid inner surface and initiate cracking. Channel arrays of tens millimeters in length and 20 nm to 200 nm in depth on a polystyrene surface were obtained in several hours. It is a promising approach for nanochannel fabrication with low cost. However, in their work, only ethanol was used and no information was given regarding how to obtain nanocracks of smaller sizes in general cases; furthermore, the channels were obtained in the form of compact arrays. Generally, the capability of making a single nanochannel is essential to investigate the transport phenomena in nanoscale.

In order to improve the nanocrack method and create single nanochannels with smaller size, this paper presents a systematic study of nanocrack formation on polystyrene surface and fabrication of single nanochannels by the nanocrack method. A series of chemical reagents including pure water, acetone, toluene, methanol, ethanol, n-propanol, isopropanol, n-butanol, sec-butanol, tert-butanol, and n-pentanol were tested. Isopropanol solutions with different concentrations were used to investigate the concentration effects. The effects on the crack size of the heating temperature ranging from 70 °C to 110 °C and the heating time ranging from 4 to 48 h were examined. The solubility parameter is used to explain the crack behavior and to predict the final crack size. Based on the experimental results and the solubility theory, a guideline for fabrication of small nanocracks on solid polymer surface is provided.

II. EXPERIMENTAL DETAILS

This paper studies the nanocrack formation on a polystyrene surface. The polystyrene petri-dishes (VWR[®], polystyrene disposable sterile) were purchased from Fisher Scientific. First, paper tapes (Avery[®]) bought from Walmart were pasted onto the petri-dish lid surface to localize a small window, with 1.5 cm in length and 5 mm in width. Second, the petri-dish lid was put onto a plastic reservoir (Evergreen Scientific, two position caps) filled with a certain volume of a chemical reagent, from 0.5 ml to 3 ml. The plastic reservoir is 17 mm in height and 19 mm in diameter. Figure 1 shows the layout of the experimental system.

In this work, the chemical reagents are pure water, acetone (99%), toluene (98.5%), and eight kinds of alcohols, i.e., methanol (99.8%), ethanol (95%), n-propanol (99.5%), isopropanol (99.5%), n-butanol (99%), sec-butanol (99%), tert-butanol (99.5%), and n-pentanol (99%). All

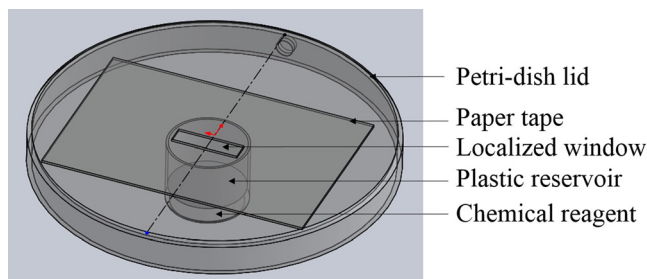


FIG. 1. General layout of the experimental system.

these chemicals were purchased from Fisher Scientific. The alcohol-water solutions were made by diluting alcohols with pure water to achieve the desired alcohol concentration. Finally, the above-mentioned assembly (the petri-dish lid on the plastic reservoir) was placed onto an electric heat plate (Torrey Pines Scientific®). The heating temperature was precisely controlled over a large range from 70 °C to 105 °C, and the heating time ranges from 4 h to 48 h. The other side of the petri-dish was open to the air, and the ambient temperature was 23–24 °C. Cracks on the petri-dish surface were inspected by using a Nikon TE2000-E microscope with a 60× objective lens or a 100 × oil objective lens. A CCD camera (purchased from Q imaging®) and the imaging analysis software (NIS-Elements BR) of the microscope were used to capture and digitize the images of the cracks. Small nanocracks and nanochannels were observed by AFM (Multimode™ SPM, Digital Instruments). Under each experimental condition, i.e., a certain temperature, a certain volume, a certain concentration, and a certain heating time, the experiments were repeated for at least three times independently, the number and the width of the cracks as well as the success rates were recorded. For a given set of conditions, if no cracks appeared in the first eight independent experiments, it is believed that the success rate is zero; otherwise, more experiments would be conducted until cracks were observed in three or more independent experiments. The average crack size was obtained by measuring different cracks for at least five times for each case.

To transfer the pattern of the nanocrack from the polystyrene surface onto PDMS slabs, technique introduced by Xu *et al.*³¹ was applied. Liquid smooth-cast 305 purchased from Sculpture Supply Canada was used to replicate the nanocracks. Part A of the liquid smooth-cast 305 was well mixed with part B of smooth-cast 305 (1:1 by volume) and degassed in a vacuum oven (Isotemp®, vacuum oven Model: 280A) at -27 in Hg for 7 min before poured it onto the polystyrene petri-dish lid surface. The next step was to place the petri-dish lid onto an aluminum plate at room temperature to prevent the smooth-cast 305 mixture from overheating, because a large amount of heat will be generated during the curing process, which would destroy the nanocracks on the polystyrene surface. After 30 min, the plastic mold was peeled off from the petri-dish lid. The cracks were transferred to the smooth-cast 305 layer, forming a positive mold (Figure 2(b)). To further solidify the positive mold, the smooth-cast 305 mold was placed into a thermal oven (Isotemp®, vacuum oven Model: 285A) at 80 °C for 1 h. Finally, a thin layer of hard PDMS³² is casted onto the positive mold followed by another thick layer of degassed PDMS (Sylgard® 184) mixture (5:1 by weight) casting to replicate the nanochannels (Figure 2(c)). The PDMS mold (Figure 2(d)) with the nanochannel was then bonded to another PDMS mold with microchannels to form the final micro-nanofluidic networks (Figure 2(e)).

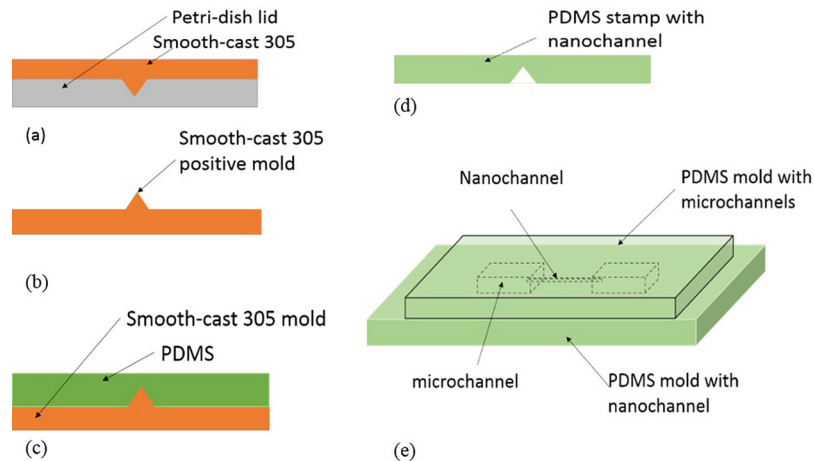


FIG. 2. Diagrams of micro-nanofluidic networks fabrication process.

III. RESULTS AND DISCUSSION

A. Solvent-induced crack mechanism

Many studies have been done to investigate solvent-induced cracks on polymer surfaces.^{33–37} Spurr and Niegisch³⁸ divided the cracking phenomena into three steps: initiation, propagation, and termination. The initiation step determines the location of individual crack, generally, cracks start at surface defects; propagation depicts the initial growth of the cracks, combining with stress releasing; and in the last step, the cracks stop growing. Moreover, cracking on polymers have to meet three conditions (a) a dilation stress field, (b) a stress greater than the critical value, and (c) a driving force for cracks to grow.³⁹ It is widely accepted that the penetration of liquid solvents into polystyrene, causing a reduction of the glass transition temperature T_g , is a key to solvent-induced cracking behavior.³⁴ The glass transition temperature of polystyrene is about 105 °C. However, the glass transition temperature of polystyrene will be reduced by tens of degree after solvent-induced swelling.⁴⁰ Kambour *et al.* discussed the mechanism of the solvent-induced cracking in detail.^{40–43} Xu *et al.*³¹ considered that the surface tension releasing on polystyrene surface due to shrinking process following surface swelling is the driving force for the cracks.

In the experiments conducted in this work, the formation of nanocracks on polystyrene surface may be divided into the following steps: First, the liquid reagent is heated into vapor which will condense and form a thin liquid membrane on the surface of the polystyrene lid due to temperature difference. Consequently, the solid polystyrene will absorb the liquid and form a swollen layer. Second, after a long time of heating, the liquid reagent is fully vaporized. The absorbed reagent will be released from the swollen layer. The swollen layer starts shrinking, which will increase the stress of the polystyrene surface. When the surface stress is larger than the critical value, cracks initiate from the defects spot to release the surface stress. The longer the heating time, the more absorbed reagent will release from the swollen layer. As a result, the surface stress becomes larger which will in turn contribute to a larger crack size, in both axial and vertical directions. Finally, the swollen layer stops shrinking when the absorbed reagent is completely released; therefore, the cracks stop growing.

The swelling process determines the thickness of the swollen layer, which affects the size of the cracks, because the swollen layer are very thin, usually 0.1 to 1 μm ,⁴⁴ and the solvent-induced cracking never occurs in the bulk layer. The swelling process is controlled by the rate of uptake of the reagent, which depends on the solubility and the diffusion coefficient. The diffusion coefficient is dependent on the temperature, concentration gradient, structure, and size of the reagent molecules. For instance, when the reagent molecule is larger or with more bulky molecular structure, the diffusion coefficient will be smaller, which will decrease the speed of the swelling process and result in a thinner swollen layer and a smaller size of cracks.

It is found that a good solvent for a specific kind of solid polymer should have a solubility parameter value close to that of the solid polymer.⁴⁵ The solubility parameter is used to describe the degree of interaction between different materials based on the molecular cohesive energy density. The solubility parameter difference between the polymers and solvent solutions can also be used to predict the critical strains during the solvent-induced crack.^{34,35,46} Hansen Solubility Parameter (HSP) is based on the “like dissolves like” principle and is applied to predict if one polymer material can be dissolved by another solution.⁴⁶ And the HSP can be divided into three parts,³⁵

$$\delta_t^2 = \delta_d^2 + \delta_p^2 + \delta_h^2, \quad (1)$$

where δ_t is the total solubility parameter, δ_d refers to the energy from nonpolar dispersion interactions, δ_p stands for energy from dipole interactions, and δ_h is the energy from interactions between hydrogen bonds. A larger difference in solubility parameters between the solvent liquid and the solid polymer indicates that a larger critical strains are required to initiate the stress cracking.⁴⁶ A larger critical strain means that the cracking process is intense, and cracks of larger sizes will be created to release the stress energy if the number of defects is limited.

B. Effect of reagents

Figure 3 compares the width of cracks obtained by exposing the polystyrene surfaces to eight kinds of alcohols with two liquid volumes, 1 ml and 2 ml, for 24 h at 90 °C. For each set of conditions, four independent experiments were performed and for each experiment, five cracks were measured at least for three times to calculate the mean size value. Apparently, from Figure 3, one can see that the width of cracks increases with the liquid alcohol volume as well as the heating temperature. The effects of the temperature and the liquid volume will be discussed in Secs. III C and III E. Here, the discussion will concentrate on the dependence of cracks on the different types of alcohols. As shown in Figure 3, cracks created by methanol are larger than that made by other alcohols, and the crack size created by tert-butanol is the smallest.

Figure 4 shows the pictures of the cracks created by heating 2 ml pure alcohols at 90 °C for 12 h. For (a) methanol, (b) ethanol, (c) n-propanol, (d) isopropanol, and (g) tert-butanol, single crack or crack arrays were generated and the width of the cracks shows a decreasing tendency from methanol, ethanol to n-propanol and finally to isopropanol. However, for (e) n-butanol, (f) sec-butanol, and (h) n-pentanol, the cracks show as massive crossing patterns.

Regarding the effects of the molecule size and polar groups of alcohols on the critical stress for solvent cracking on the surface of polystyrene, Narisawa⁴⁷ reported that alcohols with bigger molecular sizes will result in larger critical stress for crack initiation on polystyrene surfaces, and polar groups in the molecules result in an increase of the critical stress as well. Iisaka⁴⁸ showed that the crack initiation energy in the solvent-induced crack on polystyrene is a function of the length of n-alcohol molecules chains, and the speed of crack initiation on polymer surface is dependent on the diffusion coefficient of the solvent molecules, and a larger diffusion coefficient will result in a smaller activation energy for a certain crack initiation. Also, Riquet *et al.*⁴⁹ proved that methanol with a smaller molecular size penetrates much faster in polystyrene than ethanol at 40 °C, and the diffusion coefficients are 1.9×10^{-9} cm²/s and 0.46×10^{-9} cm²/s for these two alcohols, respectively. Compared with methanol and ethanol, the diffusion coefficient for isopropanol in polystyrene is much smaller, 0.2×10^{-9} cm²/s.⁴⁹

As discussed above, both the solubility parameter and the diffusion coefficient affect the crack formation. The total solubility parameter has taken the polarity, hydrogen bonds, and dispersion interactions into account. With respect to the diffusion effect, since the temperature and the concentration gradient are identical for all the cases, only the molecular size should be considered. The molecular size can be expressed in terms of molecular volume. Table I shows the Hansen solubility parameter and the molecular volume of the reagents used in this study.

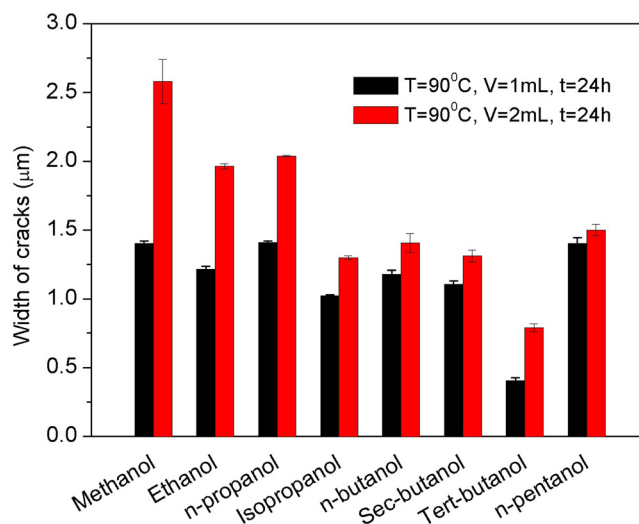


FIG. 3. Width of the cracks fabricated by heating different kinds of alcohols after 24 h; the heating temperature: $T = 90$ °C, and liquid volume: $V = 1$ ml and 2 ml.

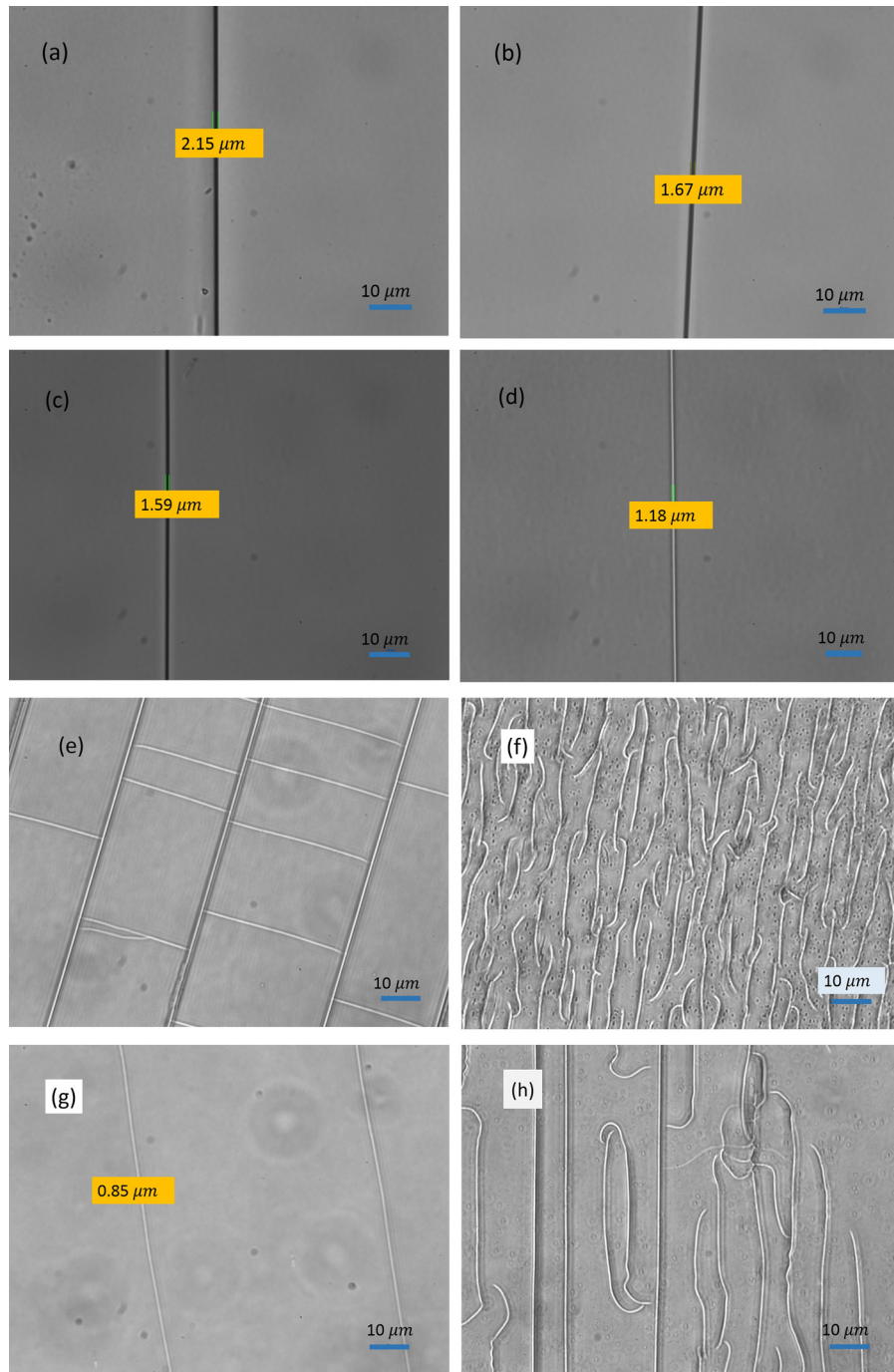


FIG. 4. 60 \times images of nanocracks on polystyrene surface fabricated by heating eight kinds of alcohol at 90 $^{\circ}$ C for 12 h, for all the cases, the alcohol volume is 2 ml. (a) methanol, (b) ethanol, (c) n-propanol, (d) isopropanol, (e) n-butanol, (f) sec-butanol, (g) tert-butanol, and (h) n-pentanol.

The solubility parameter of polystyrene is 20.0 (J/cm 3) $^{1/2}$. If diffusion coefficient is not taken into account, water with a solubility parameter of 47.8 (J/cm 3) $^{1/2}$ is the weakest solvent to polystyrene (the solubility parameter difference is 27.8 (J/cm 3) $^{1/2}$), while acetone with a solubility parameter of 19.9 (J/cm 3) $^{1/2}$ is the strongest solvent for polystyrene (the solubility parameter difference is 0.1 (J/cm 3) $^{1/2}$) in the swelling process. Acetone and toluene have been used to swell polystyrene surface and fabricate nanocracks; however, they are too strong and polystyrene can

TABLE I. Solubility parameters and molecular volume of alcohols.^{44,48-51} The unit of δ_t , δ_d , δ_p , and δ_h is $(\text{J}/\text{cm}^3)^{1/2}$, and the unit of molecular volume is cm^3/mol .

Alcohols	δ_t	δ_d	δ_p	δ_h	Molecular volume
Methanol	29.7	15.1	12.3	22.3	40.7
Ethanol	26.6	15.8	8.8	19.4	58.5
n-propanol	24.5	16.0	6.8	17.4	75.2
Isopropanol	23.5	15.8	6.1	16.4	76.8
n-butanol	23.1	16.0	5.7	15.8	91.5
sec-butanol	22.2	15.8	5.7	14.5	92.0
tert-butanol	21.8	15.2	5.1	14.7	95.7
n-pentanol	21.6	15.9	4.5	13.9	108.6
Polystyrene	20.0	17.6	6.0	3.9	...
Acetone	19.9	15.5	10.4	7.0	74.0
Toluene	18.2	18.0	1.4	2.0	106.8
Water	47.8	15.5	16.0	42.3	18.0

be dissolved in these reagents rapidly. By contrast, water is too weak, and no crack is generated on the polystyrene surface after a 48-h heating of 3 ml pure water at 90 °C.

As shown in Table I, for the alcohols, it is clear that the difference of solubility parameter between polystyrene and the alcohols decreases with the increasing molecular volume, i.e., methanol, ethanol, n-propanol, isopropanol, n-butanol, sec-butanol, tert-butanol, and n-pentanol, from large to small. Interestingly, from Figure 3, one can see that the width of cracks is also showing the same decreasing tendency roughly, except for n-pentanol, because the molecule of n-pentanol is too large, and it is hard for polystyrene to absorb the big molecules to initiate cracks uniformly.

In addition, for the isomers (alcohols with identical molecular formulas but different molecular structures), such as n-propanol and isopropanol, as well as n-butanol, sec-butanol, and tert-butanol groups, the molecular volumes show little effects on the crack formation, and the swelling process is mainly dependent on their solubility parameters. For instance, cracks created by n-propanol are larger than that created by isopropanol due to the bigger solubility parameter difference between n-propanol and polystyrene, $4.5 (\text{J}/\text{cm}^3)^{1/2}$, compared with that in the case of isopropanol, $3.5 (\text{J}/\text{cm}^3)^{1/2}$. A larger solubility parameter difference will contribute to a larger critical strain and a larger crack size, and a smaller difference of solubility parameters makes a smaller critical strain as well as a smaller crack size. However, when the critical strain is too small, crossing cracking and amorphous dissolved patterns will appear. For example, the solubility parameters of n-butanol, sec-butanol, and n-pentanol are too close to that of polystyrene, which makes the initiation of cracks easily, and crossing patterns appear after the swelling process (see Figure 4).

Therefore, the criteria for selecting a strong cracking reagent will include: (a) a solubility parameter value close to that of polystyrene and (b) a small molecular volume, or both. However, when the reagent is too strong, crossing cracks will be generated. A proper reagent for nanocrack fabrication should be a chemical which does not swell the polymer greatly; in other words, the solvent should have a considerable solubility parameter value difference from that of the solid polymer, and an appropriate molecular size. Therefore, considering these two factors, isopropanol is a proper agent to study the cracking on polystyrene surfaces. In the following studies, isopropanol is chosen as the testing liquid to systematically study the diffusion effects, such as heating temperature, heating time, concentration, and liquid volume.

C. Effects of alcohol volume and the heating time

The volume of the liquid reagents affects the contacting time between the reagent liquids and the polystyrene surface directly in the swelling process when the heating temperature is constant. At a given heating temperature, a larger quantity of alcohol takes a longer time to

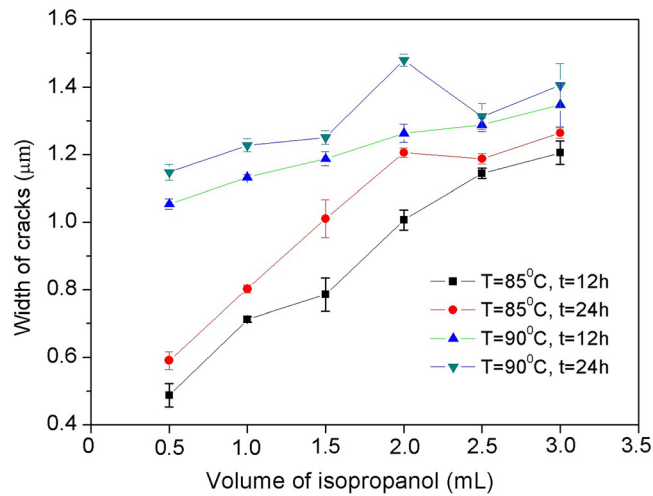


FIG. 5. Volume effects on crack size. A certain volume of isopropanol (99.5%), from 0.5 ml to 3 ml, is heated at a fixed temperature, 85 °C and 90 °C, for 12 h and 24 h.

fully vaporize, which means a longer contacting time of the polystyrene surface with the alcohol. Consequently, a larger quantity of reagent molecules will diffuse into the polystyrene, and the swollen layer will be thicker, and the final crack size will be larger. During the experimental process, all the reagent liquids were fully vaporized before inspection. Figure 5 presents the width of cracks fabricated by heating different quantities (from 0.5 ml to 3 ml) of isopropanol at 85 °C and 90 °C for 12 h and 24 h. The results show that the crack size increases gradually with the volume under a given temperature and a given heating time. As shown in this figure, under the condition of $T=85^{\circ}\text{C}$ and $t=12\text{h}$, the cracks obtained are about $0.5\ \mu\text{m}$ wide when the volume of the liquid alcohol is 0.5 ml, and the crack width increases almost linearly with the volume of the liquid alcohol to $1.15\ \mu\text{m}$, when the volume is 3 ml. Similarly, under the condition of $T=90^{\circ}\text{C}$ and $t=12\text{h}$, the width of the cracks increases from about $1.05\ \mu\text{m}$ to almost $1.3\ \mu\text{m}$ when the volume increases from 0.5 ml to 3 ml. Also seen from Figure 5, a higher temperature generates a larger crack size under the same liquid alcohol volume. More discussion about the temperature effects will be provided in Sec. III E.

The heating time is an essential parameter for the solvent crack process, including swelling, reagent releasing, crack initiation, and crack growth. The longer the reaction time, the larger stress will be generated, which will in turn result in a larger crack size. Figure 6 shows the

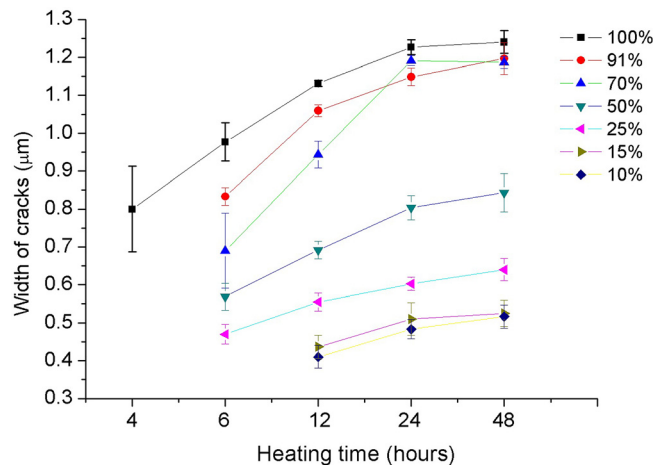


FIG. 6. Increase of crack size with time. For all the cases, the heating temperature is 95 °C, the heating time is from 4 h to 48 h, and the volume of isopropanol solutions is 1 ml.

heating time effects on the crack size, under a constant heating temperature of 95 °C and a constant liquid alcohol volume of 1 ml. Isopropanol solutions of seven different concentrations ranging from 5% to 99.5% were tested. From the figure, one can see that the width of the cracks increases with time for all the concentrations. However, it takes longer time for the cracks to initiate when the concentration becomes lower. Specifically, only about 4 h are needed for the case of 99.5% concentration to initiate cracks. By contrast, in the cases of 10% and 15% concentrations, the cracks appear generally after 12 h of heating. Moreover, it is obvious that the increase of the crack width becomes slower after 24 or 48 h and the crack size is likely to level off after heating for 48 h, because the absorbed isopropanol molecules are fully released from the swollen layer, and no more stress release is needed by enlarging the crack size. Figure 7 presents the crack initiation process. From the picture, we cannot see any crack at 4 h. After another 2 h, a crack grows on a defect spot and becomes longer in half an hour. However, the width of the crack shows little change.

D. Concentration effects and the role of water

Isopropanol solutions with different concentrations from 5% to 99.5% were used to study the concentration effects on nanocrack formation. Figure 6 also shows the dependence of the width of the cracks on the concentration of isopropanol solutions. It is clear that the crack size increases with the concentration. In Figure 6, the smallest crack size obtained is about 0.4 μm , under the condition of heating 1 ml 10% isopropanol solution at 95 °C for 12 h. In addition, there were no cracks when the concentration is very low, for example, lower than 10%. This is because no sufficient isopropanol molecules penetrate into the polystyrene surface, and the swollen layer is too thin to initiate cracks.

As discussed above, the solubility parameter of water is 47.8 $(\text{J}/\text{cm}^3)^{1/2}$, which is far from the solubility parameter of polystyrene, 20 $(\text{J}/\text{cm}^3)^{1/2}$, one can conclude that water is a weak reagent for the initiation of cracking on polystyrene. In this study, pure water was also examined to see if it could create cracks on polystyrene surfaces. For example, polystyrene surfaces were exposed to 3 ml pure water at 85 °C for 48 h. However, there were no cracks on polystyrene surfaces. Therefore, it was concluded that water is too weak to swell polystyrene and initiate the cracking process.

However, for water-alcohol mixtures, water plays an important role in the formation of small cracks on polystyrene surfaces. On the one hand, the boiling point of water is higher than

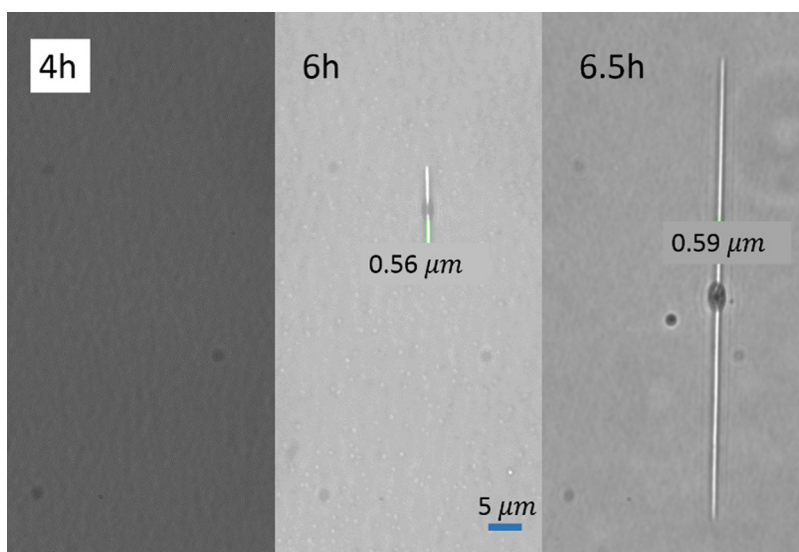


FIG. 7. Initiation of a nanocrack on polystyrene surface (60 \times microscope image). The working condition is heating 1 ml 50% isopropanol solution at 95 °C.

that of isopropanol, and the isopropanol vapor will dissolve in the condensed water film on the polystyrene surface, which will prolong the contacting time of isopropanol with the polystyrene surface and increase the quantity of isopropanol penetrating into the polystyrene at the same time. On the other hand, according to Fick's law, a lower concentration of isopropanol, due to the water film, will decrease the concentration gradient in the liquid-solid boundary, which will slow down the diffusion process. As a consequence, the quantity of isopropanol penetrated into the swollen layer will be smaller, leading to a thinner swollen layer and a smaller crack size. During the isopropanol releasing process, the water film on the polystyrene surface acts like a "buffering" layer, which will reduce the concentration gradient and make the releasing process smooth.

E. Temperature effects

As discussed before, the temperature is a key factor in the process of crack formation. There will be no cracks when the temperature is lower than the glass transition temperature of the solid polymer. Also, a lower temperature means a lower diffusion coefficient. Figure 8 shows the temperature effects on the crack size. In Figure 8, the temperature ranges from 70 °C to 105 °C, and the concentration of isopropanol solutions is from 10% to 99.5%. For all the cases, the heating time is 24 h and the volume is 2 ml. It is clear that the width of the cracks increases with the temperature and when the temperature is lower than 70 °C, no crack appears at all. When the temperature is higher than 105 °C, cross-cracking appears. Under the same condition, tests of a smaller reagent volume (1 ml) were conducted, and the results show the same tendency. Figure 9 shows the smallest crack of 320 nm width obtained by heating 1 ml 25% isopropanol solution at 80 °C for 12 h. The picture was taken by using a 100× oil lens, and the tiny winkles on the surface were caused by the reaction between the immersion oil and the polystyrene surface.

It should be noted that nanocracks may not always form in every experiments, because the nanocrack formation depends largely on the existence of defects on the surface. It is extremely hard to initiate cracks when there are no defects on the polystyrene surface even though the stress is large. According to the statistics of the experimental results in this study, generally, the success rate of forming cracks increases with temperature as well as the volume and concentration of alcohol solutions. For example, for the cases of 1 ml, 2 ml, and the 24-h heating, when the temperature is lower than 75 °C, the success rate of forming cracks is very low (<15%), and small cracks can only be obtained by chance. However, when the temperature is

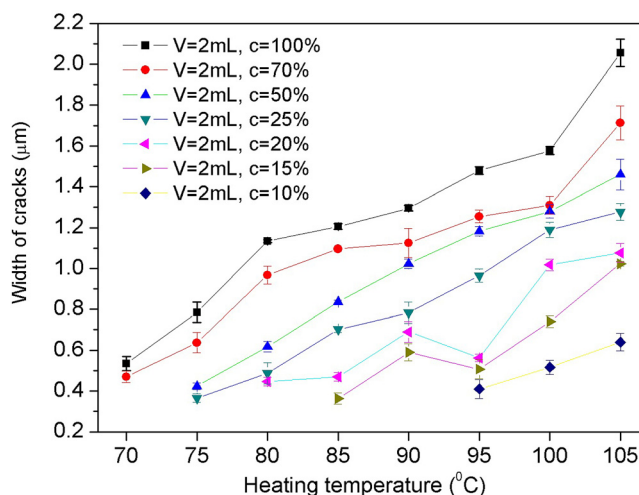


FIG. 8. Temperature effects on crack size. The temperatures are 70 °C, 75 °C, 80 °C, 85 °C, 90 °C, 95 °C, 100 °C, and 105 °C, and the concentration of the isopropanol solutions is from 10% to 99.5%; the heating time is 24 h and the volume is 2 ml.

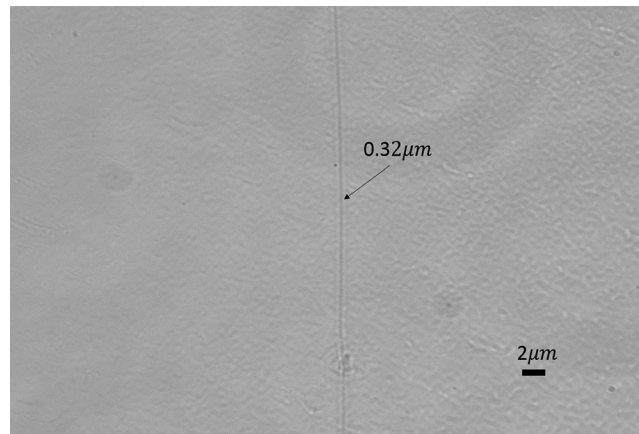


FIG. 9. 100 \times image of 320 nm wide nanocrack on polystyrene surface. The creation condition is: $T = 80^\circ\text{C}$, $C = 25\%$ isopropanol, $t = 12\text{ h}$, and $V = 1\text{ ml}$.

higher than 105°C , crossing cracks are created. For $80^\circ\text{C} < T < 100^\circ\text{C}$, the success rate of forming cracks is generally higher than 50%, even approaches 100% when the concentration of alcohol is higher than 15%. It is also very hard to initiate cracking when the concentration of alcohol is too low. For instance, essentially no cracks appear when the concentration is lower than 5%. However, the success rate at low concentration can still be enhanced by increasing the volume of alcohol solutions or increasing the heating temperature, or both. All in all, though it is hard to obtain small cracks every time, the success rate can be controlled by adjusting the experimental conditions.

F. Number of nanocracks

Fabrication of a single nanochannel is essential for the nanofluidic studies. When multiple nanocracks are very close to each other, it is impossible to use them to make a single nanochannel and connect such a nanochannel with a single microchannel. In the experiments conducted in this work, the total number of the cracks formed in the small window (as illustrated in Figure 1) was recorded. Figure 10 show the number of the cracks created by heating 1 ml and 2 ml isopropanol solutions at various temperatures for 24 h. From Figures 10(a) and 10(b), one can see that the number of the cracks increases rapidly with the concentration when the concentration value is lower than 70%. However, when the concentration is higher than 70%, the number of cracks decreases. Moreover, when the concentration is lower than 15%, the number of cracks is generally smaller than 5. Though the cracks are not uniformly distributed, the

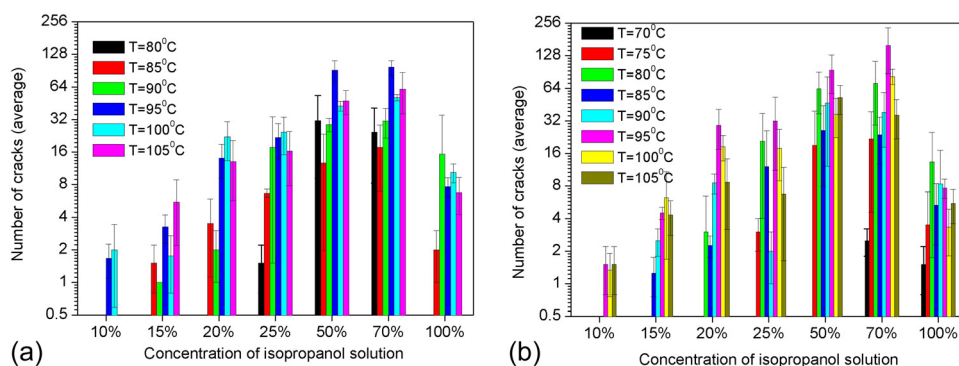


FIG. 10. Number of nanocracks. The temperatures are 70°C , 75°C , 80°C , 85°C , 90°C , 95°C , 100°C , and 105°C , and the concentration of the isopropanol solutions is from 10% to 99.5%; the heating time is 24 h and the volumes are (a) 1 ml and (b) 2 ml, respectively.

distance between the cracks is generally larger than $500\ \mu\text{m}$, even $1\ \text{mm}$, large enough for a connection with a microchannel. In fact, in many cases, only a single crack appeared. It is credible that this method can be used to fabricate single nanocracks.

G. Fabrication of smaller nanocracks

Enlightened by the results of the systematic studies described above and particularly the results shown in Figure 3, tert-butanol was selected to create smaller nanocracks on polystyrene surfaces, because the solubility parameter of tert-butanol ($21.8\ (\text{J}/\text{cm}^3)^{1/2}$) is closer to that of polystyrene ($20(\text{J}/\text{cm}^3)^{1/2}$) than the solubility parameter of isopropanol ($23.5(\text{J}/\text{cm}^3)^{1/2}$) (see Table I), and the molecular size of tert-butanol is not too large. According to the guideline mentioned above, the next step was to find an appropriate condition of crack formation. First, 1 ml of 75%, 50%, 25%, and 15% tert-butanol solutions was chosen to generate nanocracks. These solutions were heated at $95\ ^\circ\text{C}$ for 24 h, then the width of the cracks was measured; the crack widths were approximately $0.63\ \mu\text{m}$, $0.37\ \mu\text{m}$, and $0.31\ \mu\text{m}$, respectively. For the case of 15% tert-butanol solution, no crack was observed at all. In order to create a smaller crack size, a lower temperature was applied. In the experiments, 1 ml 20% tert-butanol solution was heated at $80\ ^\circ\text{C}$ for 8 h, and smaller nanocracks could be obtained. For example, as shown in Figure 11(a), the left is the 3-D AFM image of a nanocrack and the right is the profile of the cross-section of the crack. The average value of the crack size is $63.72\ \text{nm}$ wide and $17.4\ \text{nm}$ deep. Fig. 11(b) shows a nanochannel fabricated on the PDMS surface by using this nanocrack, following the process described in the experimental section. The size of the nanochannel is similar to that in Fig. 11(a), with average value of $59.86\ \text{nm}$ in width and $10.27\ \text{nm}$ in depth. Comparing these values, one can see that the size of the final PDMS nanochannels is smaller than that of the nanocrack, because it is hard to fully fill the triangle shape nanocrack with viscous liquid smooth-cast, which will result in a smaller size positive mold and a smaller nanochannel on PDMS. In addition, from Figures 11(a) and 11(b), one can also see that the surface of the polystyrene is much smoother than that of the PDMS, because the liquid smooth-cast can

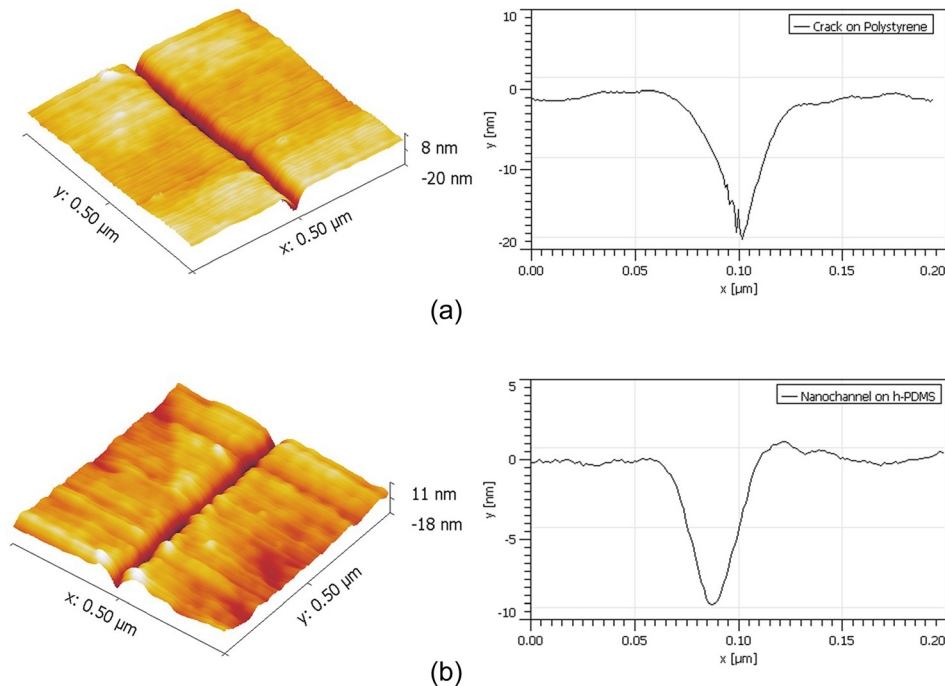


FIG. 11. (a) AFM image and the cross-section profile of a $63.72\ \text{nm}$ wide and $17.40\ \text{nm}$ deep nanocrack created by heating 1 ml 20% tert-butanol solution at $80\ ^\circ\text{C}$ for 8 h. (b) AFM image and the cross-section profile of a nanochannel replicated from this nanocrack, the size of the channel is $59.86\ \text{nm}$ wide and $10.27\ \text{nm}$ deep.

also swell the polystyrene surface, which makes the PDMS surface not so smooth. A lower Young's module of the h-PDMS also contributes to the roughness during the AFM measurement.

IV. CONCLUSION

A systematic experimental study was performed to investigate the formation of nanocracks on polystyrene surfaces. The solubility parameter and the diffusion coefficient were taken into account in the solvent-induced crack mechanism. A proper solubility parameter difference and an appropriate reagent molecule size are essential factors for the swelling and cracking process. The thickness of the swollen layer and the critical strain dominate the size of cracks. The size of cracks increases with heating temperature, heating time, volume, and concentration of alcohol solutions. In order to obtain a single nanocrack with a smaller crack size, the first step is to choose a proper reagent that has a solubility parameter close to the solid polymer (e.g., polystyrene) and a relatively large molecule size. The next step is to control the swelling and cracking processes with a low reagent concentration, a low temperature, a short heating time, and a small reagent volume. In this work, cracks with a width as small as 63.72 nm wide and 17.4 nm deep were created on polystyrene surfaces by heating 20% tert-butanol solution at 80 °C for 8 h. Single nanochannels were replicated by using these small nanocracks onto PDMS slabs successfully. Although the experimental studies presented in this paper are limited by the specific set of the chemical reagents and the solid polymer (polystyrene), the general conclusion can be used to guide future studies of nano-crack formation using other reagents and solid polymers.

ACKNOWLEDGMENTS

The authors wish to thank the financial support of the Natural Sciences and Engineering Research Council (NSERC) of Canada through a research grant to Dr. Li.

- ¹A. Plecis, R. B. Schoch, and P. Renaud, *Nano Lett.* **5**, 1147 (2005).
- ²R. Karnik, R. Fan, M. Yue, D. Li, P. Yang, and A. Majumdar, *Nano Lett.* **5**, 943 (2005).
- ³Q. Pu, J. Yun, H. Temkin, and S. Liu, *Nano Lett.* **4**, 1099 (2004).
- ⁴P. Chen, J. Gu, E. Brandin, and Y. Kim, *Nano Lett.* **4**, 2293 (2004).
- ⁵H. Liu, J. He, J. Tang, H. Liu, P. Pang, D. Cao, P. Krstic, S. Joseph, S. Lindsay, and C. Nuckolls, *Science* **327**, 64 (2010).
- ⁶G. F. Schneider and C. Dekker, *Nat. Biotechnol.* **30**, 326 (2012).
- ⁷S. Prakash, A. Piruska, and E. Gatimu, *IEEE Sensors J.* **8**, 441 (2008).
- ⁸R. Schoch, J. Han, and P. Renaud, *Rev. Mod. Phys.* **80**, 839 (2008).
- ⁹C. Vieu, F. Carcenac, A. Pepin, and Y. Chen, *Appl. Surf. Sci.* **164**, 111 (2000).
- ¹⁰V. R. Manfrinato, L. Zhang, D. Su, H. Duan, R. G. Hobbs, E. A. Stach, and K. K. Berggren, *Nano Lett.* **13**, 1555 (2013).
- ¹¹L. D. Menard and J. M. Ramsey, *Nano Lett.* **11**, 512 (2011).
- ¹²A. A. Tseng, *J. Micromech. Microeng.* **14**, R15 (2004).
- ¹³A. F. G. Leontowich and A. P. Hitchcock, *Appl. Phys. A* **103**, 1 (2011).
- ¹⁴B. J. Lin, *J. Vac. Sci. Technol.* **12**, 1317 (1975).
- ¹⁵M. J. O'Brien, P. Bisong, L. K. Ista, E. M. Rabinovich, A. L. Garcia, S. S. Sibbett, G. P. Lopez, and S. R. J. Brueck, *J. Vac. Sci. Technol., B: Microelectron. Nanometer Struct.* **21**, 2941 (2003).
- ¹⁶S. Y. Chou, *J. Vac. Sci. Technol., B: Microelectron. Nanometer Struct.* **15**, 2897 (1997).
- ¹⁷Q. Xie, Q. Zhou, F. Xie, J. Sang, and W. Wang, *Biomicrofluidics* **6**, 016502 (2012).
- ¹⁸W. Sparreboom, J. Eijkel, J. Bomer, and A. Van Den Berg, *Lab Chip* **8**, 402 (2008).
- ¹⁹B. J. Hinds, N. Chopra, T. Rantell, R. Andrews, V. Gavalas, and L. G. Bachas, *Science* **303**, 62 (2004).
- ²⁰W. Gong, J. Xue, Q. Zhuang, X. Wu, and S. Xu, *Nanotechnology* **21**, 195302 (2010).
- ²¹S. H. Park, H.-J. Shin, Y.-H. Kim, D.-Y. Yang, J.-C. Lee, and S. Lee, *J. Micromech. Microeng.* **22**, 095019 (2012).
- ²²S. Park and Y. Huh, *Proc. Natl. Acad. Sci. U. S. A.* **106**, 15549 (2009).
- ²³J. Lee, Y. Yoon, J. Kim, Y. Kim, and K. Jo, *Bull. Korean Chem. Soc.* **32**, 33 (2011).
- ²⁴D. Huh, K. L. Mills, X. Zhu, M. A. Burns, M. D. Thouless, and S. Takayama, *Nat. Mater.* **6**, 424 (2007).
- ²⁵B. Kim, J. Heo, H. Kwon, S. Cho, J. Han, S. Kim, and G. Lim, *ACS Nano* **7**, 740 (2013).
- ²⁶P. Sivanesan, K. Okamoto, and D. English, *Anal. Chem.* **77**, 2252 (2005).
- ²⁷J. Li, C. Liu, X. Ke, Z. Xu, Y. Duan, Y. Fan, and M. Li, *Lab Chip* **12**, 4059 (2012).
- ²⁸A. Grimes, D. N. Breslauer, M. Long, J. Pegan, L. P. Lee, and M. Khine, *Lab Chip* **8**, 170 (2008).
- ²⁹X. Zhu, K. L. Mills, P. R. Peters, J. H. Bahng, E. H. Liu, J. Shim, K. Naruse, M. E. Csete, M. D. Thouless, and S. Takayama, *Nat. Mater.* **4**, 403 (2005).
- ³⁰N. Bowden, W. T. S. Huck, K. E. Paul, and G. M. Whitesides, *Appl. Phys. Lett.* **75**, 2557 (1999).
- ³¹B.-Y. Xu, J.-J. Xu, X.-H. Xia, and H.-Y. Chen, *Lab Chip* **10**, 2894 (2010).
- ³²H. Schmid and B. Michel, *Macromolecules* **33**, 3042 (2000).
- ³³H. Brown, *Polymer (Guildf)* **19**, 1186 (1978).

- ³⁴C. H. M. Jacques and M. G. Wyzgoski, *J. Appl. Polym. Sci.* **23**, 1153 (1979).
- ³⁵C. M. Hansen, *Polym. Degrad. Stab.* **77**, 43 (2002).
- ³⁶B. Earl, R. Loneragan, and M. Crook, *J. Mater. Sci.* **8**, 370 (1973).
- ³⁷V. Kefalas and A. Argon, *J. Mater. Sci.* **23**, 253 (1988).
- ³⁸O. Spurr and W. Niegisch, *J. Appl. Polym. Sci.* **VI**, 585 (1962).
- ³⁹S. Sternstein and L. Ongchin, *Polym. Prepr.* **10**, 1117 (1969).
- ⁴⁰R. P. Kambour, C. L. Gruner, and E. E. Romagosa, *J. Polym. Sci., Polym. Phys. Ed.* **11**, 1879 (1973).
- ⁴¹R. P. Kambour, *J. Polym. Sci., Part D: Macromol. Rev.* **7**, 1 (1973).
- ⁴²R. P. Kambour, C. L. Gruner, and E. E. Romagosol, *Macromolecules* **7**, 248 (1973).
- ⁴³R. Kambour and S. Smith, *J. Polym. Sci., Polym. Phys. Ed.* **20**, 2069 (1982).
- ⁴⁴J. Hoare and D. Hull, *Philos. Mag.* **26**, 443 (1972).
- ⁴⁵A. Barton, *Chem. Rev.* **75**, 731 (1975).
- ⁴⁶C. M. Hansen and L. Just, *Ind. Eng. Chem. Res.* **40**, 21 (2001).
- ⁴⁷I. Narisawa, *J. Polym. Sci., Part A-2: Polym. Phys.* **10**, 1789 (1972).
- ⁴⁸K. Iisaka, *J. Polym. Sci., Polym. Phys. Ed.* **17**, 791 (1979).
- ⁴⁹A. M. Riquet, V. Bose, and A. Feigenbaum, *Food Addit. Contam.* **18**, 165 (2001).
- ⁵⁰C. M. Hansen, *Hansen Solubility Parameters: A User's Handbook*, 2nd ed. (CRC Press, 2012).
- ⁵¹M. S. Seehra, M. Yalamanchi, and V. Singh, *Polym. Test.* **31**, 564 (2012).